LITERATURE CITED

1. Yu. A. Tadol'der, "Some quantitative trends in wear of technically pure metals," Trans. Tallin Polytech. Inst., Ser. A, No. 237 (1966).
2. Yu. V. Polezhaev and F. B. Yurevich, Thermal Treatment [in Russian], Énergiya, Moscow (1976).
3. Yu. V. Polezhaev, V. P. Romanchenkov, I. V. Chirkov, and V. N. Shebeko, "A model for calculating the erosion of a composite material," Inzh.-Fiz. Zh., 37, No. 3 (1979).
4. F. S. Harris, AIAA Paper (1975), p. 75.

A MODEL FOR CALCULATING THE EROSION OF A COMPOSITE MATERIAL

Yu. V. Polezhaev, V. P. Romanchenkov, I. V. Chirkov, and V. N. Shebeko

UDC 532.525.6.011.55.011.6

We generalize experimental data and present a model for calculating the erosion of some composite materials subject to impact by solid particles.

By the "erosion" of a material (an "obstacle") we mean a process in which the mass of the material is carried away under the action of a stream of particles impinging upon it. The erosion of a body immersed in a high-speed flow of a gas-particle mixture (so-called two-phase flow) is affected thermochemically at the expense of heat and mass transfer in the gaseous boundary layer. In order to separate these two processes we concentrate our attention, in the present paper, on two-phase flows over bodies with flow speeds less than 2000 m/sec or with temperature due to drag not exceeding typical values of body surface temperatures arising from "pure" thermochemical decomposition (2000°K for quartzitic glass composites).

Despite this limitation, we need to analyze, where possible, a wider range of interaction rates in order to observe how the dynamics of the material decomposition mechanism changes, beginning with the region of influence of elastic forces and ending with the effects of high-speed impact. A large number of experimental and computational papers (see, e.g., [1]) have been devoted to the study of high-speed impact of single particles. As the lower limit of the range of high-speed impact, the authors of these papers assume a speed V_p for which a pressure is generated at the point of contact of the particle and obstacle which is significantly higher than the flow limit under compression for both materials. In the case of colliding metals this situation already applies for $V_p \geq 1000$ m/sec.

Unfortunately, the majority of the papers published are devoted to the study of the high-speed collision of homogeneous materials, mainly, the impact of a metallic particle onto a metallic target. Many authors note, however, that in the case of high-speed impact the target material parameters of primary significance are the hardness and the density [2]. The most interesting result to be noted here is the practically linear dependence of the mass G_{er} of the target material eroded away on the kinetic energy of the particle $(G_p V_p^2/2)$. In Fig. 1 we show the experimental data from [1] for the case of the impact of steel particles onto a lead target.

In contrast to the impact of a single particle, in the case of multiple impacts each previous particle not only carries away some mass of target material but also changes the properties of the layer of target material remaining; moreover, during the impact interaction waves of compression and rarefaction propagate in this layer. In particular, even in the case of impact by micron-sized particles on a homogeneous material (quartz), numerous microcracks and spalls appear [3]. This complicates the use of arbitrary parameters relating to the initial material, such as hardness, elasticity modulus, etc., when treating experimental data for the case of multiple impact.

Parameters used in the case of single impact (crater volume, depth of penetration, etc.), which are of frequent occurrence in the literature, cannot be used for treating experimental data relating to multiple impact. A more accurate and more preferred parameter in this case is the damage intensity parameter $\bar{G}$, defined as the ratio of the outflow G_{er} of eroded material to the specific particle flux G_p reaching the target surface.

Translated from Inzhenerno-Fizicheskii Zhurnal, Vol. 37, No. 3, pp. 395-404, September, 1979. Original article submitted February 9, 1979.

0022-0841/79/3703-1011$07.50

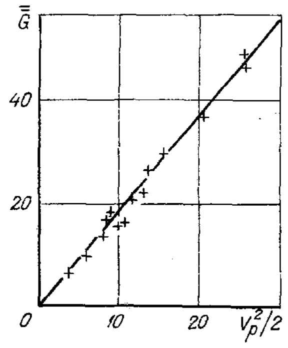

Fig. 1. Dependence of a lead target erosion intensity on the specific kinetic energy of steel particles, V_p km/sec.

We recall that in the investigation of thermochemical decomposition, presented in [4], there was introduced a very convenient energy characteristic of the process, viz., the effective damage enthalpy

$$I_{\text{eff}} = \frac{(\alpha/c_p)_0 (I_e - I_w) - \varepsilon\sigma T_w^4}{G_k},$$

where $q_0 = (\alpha/c_p)_0(I_e - I_w)$ is the convective heat flux to the surface; I_e, enthalpy of the decelerated flow; I_w, enthalpy of the gas at the wall; G_k, efflux of eroded material; $\varepsilon\sigma T_w^4$, return radiation from the damaged surface; and $(\alpha/c_p)_0$, heat-transfer coefficient. For large speeds of the incident flow the numerator of this expression can be simplified to $(\alpha/c_p)_0 I_e \approx (\alpha/c_p)_0 U_\infty^2/2$, and then the effective enthalpy turns out to be equal to the ratio of the specific kinetic energy of the gas stream to the dimensionless thermochemical damage rate $\bar{G}_k = G_k/(\alpha/c_p)_0$:

$$I_{\text{eff}} \to \frac{(\alpha/c_p)_0 U_\infty^2}{2G_k} = \frac{U_\infty^2}{2\bar{G}_k}. \tag{1}$$

Upon forming an energy balance for the erosion damage process, we can introduce, by analogy with (1), an effective enthalpy of the mass eroded away, viz.,

$$H_{\text{er}} = (G_p V_p^2)/(2G_{\text{er}}) = V_p^2/(2\bar{\bar{G}}). \tag{2}$$

This parameter characterizes the erosional firmness of the target material. In accordance with the experimental data relating to the high-speed impact of single particles onto a metallic target [1], the quantity H_{er} does not depend on the speed V_p and is, in the main, determined by the ratio of the hardness H_{B_0} of the target material to its density ρ_0:

$$H_{\text{er}} \propto (H_{B_0}/\rho_0).$$

We consider now the nature of the change in the process of the particle's interaction with the target as the speed V_p increases. To a first approximation we can identify, in turn, three interaction mechanisms which apply for small, moderate, and high-impact speeds, respectively.

1) elastic compression of the material of the target and of the particle, but with no crater formation or erosion damage;

2) formation of local zones of plastic deformation; formation of craters and of microcracks in the target material;

3) plastic flow of the target and particle materials takes place, resembling somewhat the penetration of a jet of one fluid into a half space filled with another fluid.

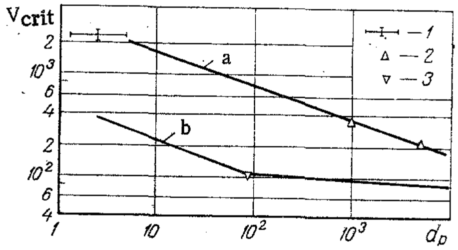

Fig. 2

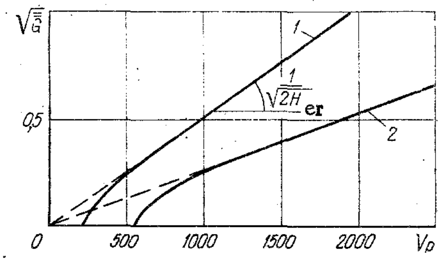

Fig. 3

Fig. 2. Variation of impact speed, critical for the onset of damage, with the size of the impacting particle for the case (a) of single particle impact, and (b) multiple particle impact. The data are for 1, a target of quartz glass, and 2, 3, target of glass Textolite. V_{crit}, m/sec; d_p, μm.

Fig. 3. Variation of the erosional damage intensity as a function of particle impact speed for different sized particles: For curve 1, $d_p = 5000$ μm; for curve 2, $d_p = 500$ μm. V_p is given in m/sec.

For brevity, we shall speak of these three interaction mechanisms as the elastic, the transitional, and the hydrodynamic phases of impact, respectively. The last of these is associated, obviously, with the phenomenon of high-speed impact, mentioned earlier.

Before going on to a mathematical description of a law describing erosional damage, we find it desirable to establish limits separating the impact speeds appropriate to the three phases.

In connection with single particle impact, we can use the theoretical and experimental data given in [5]; here, the pressure at the point of contact of the particle with the target material at the beginning of the transitional phase is close to the flow limit σ_T for uniaxial strain of the target material, while, at the end of the transitional phase the pressure is more than 3 times σ_T.

If we denote the lower limit of the transitional phase by $V_p = V_{crit}$, we can calculate it from the condition that the kinetic energy of the particle, $G_p V_p^2/2$, is converted into work of overcoming the elastic forces in the target material. Hence, we obtain

$$V_{crit} \backsim \sqrt{\sigma_T/\rho_p}. \tag{3}$$

However, if we use experimental data for millimeter-sized particles to support our calculations relative to (3), we obtain agreement with [3] with respect to V_{crit} for micron-sized particles. This circumstance compels us to revise the law for the variation of the speed V_{crit} with the particle size in the following way (see Fig. 2):

$$V_{crit} \backsim (\sigma_T/\rho_p)^{0,5} d_p^{-0,3}. \tag{4}$$

Very likely, it is this fact which gives rise to the so-called "scale effect," concerning which there are many points of view (see [6]).

In accordance with the earlier remarks relating to the pressure on the surface at the point of contact of the particle with the target material, we can estimate the upper limit of the transitional phase of the impact process as $V_p = 2V_{crit}$. Thus, we postulate an equal extent of the elastic and transitional phases on the velocity scale.

A law to describe damage due to erosion must, apparently, be a relationship which takes into account the impact speed and the particle size, but also a number of physical parameters characterizing the target and particle materials. It is also desirable that this law have a single mathematical description for the transitional and hydrodynamic phases for both single and multiple impacts. The following equation for the relative erosional damage intensity $\bar{\bar{G}}$ meets these requirements:

$$\bar{\bar{G}} = \frac{V_p^2}{2H_{er}}\left[1 - \exp\left(\frac{V_{crit} - V_p}{0.5V_{crit}}\right)\right]. \tag{5}$$

The form of the function $\bar{\bar{G}}(V_p)$ is shown in Fig. 3 for various values of H_{er} and V_{crit}.

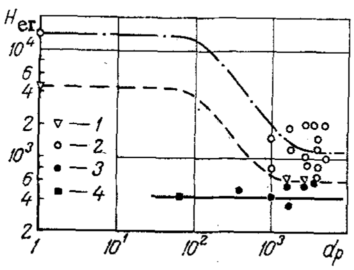

Fig. 4

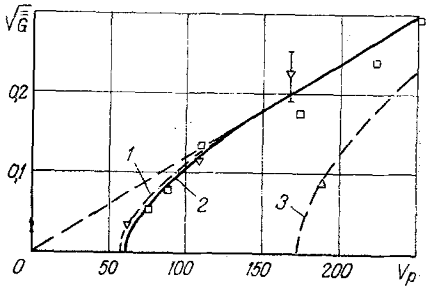

Fig. 5

Fig. 4. Variation of the effective erosional damage enthalpy as a function of particle size for the case of single impact (open data points) and multiple impact (solid data points). Data points 1 are for iron impacts onto aluminum with $3 < V_p < 10$ km/sec. For silicate particles impacting onto glass Textolite, the data points 2 are for $0.7 < V_p < 4$ km/sec and the data points 3 are for $V_p > 1$ km/sec. Data points 4 are for corundum particles impacting glass Textolite for $V_p > 1.0$ km/sec. Units for H_{er} are kJ/kg; units for d_p are μm.

Fig. 5. Comparison of the experimental and calculated erosional damage intensity data for various particle speeds, sizes, and densities. For curve 1, $d_p = 140$ μm and $\rho_p = 2500$ kg/m³; for curve 2, $d_p = 90$ μm and $\rho_p = 3900$ kg/m³; for curve 3, $d_p = 20$ μm and $\rho_p = 2500$ kg/m³.

The relation (5) reflects two fundamental aspects of a computational model of the damage process which hold for both single and multiple impacts of particles with a target.

I. The erosion damage energy of the target material (or the effective enthalpy) H_{er} does not depend on the particle impact speed V_p (this, however, does not eliminate the dependence of H_{er} on other parameters such as particle size d_p and collisional frequency n).

II. In the transitional phase of the impact process, the start and extent of which are determined by the parameter V_{crit} (see the equations in [4]), the dependence of the relative erosional damage intensity $\bar{\bar{G}}$ on the speed V_p, as well as on the size and density of the particles, is substantially stronger than in the hydrodynamic phase.

For $V_p > 2V_{crit}$ the relation (5) goes over into the simpler equation (2), which can be used for the experimental determination of H_{er}. The closer the range of the experimental studies is to V_{crit}, the higher are the degrees of the approximate formulas for the dependence of $\bar{\bar{G}}$ on V_p.

In Fig. 4 we present experimental data showing how the effective erosional damage enthalpy H_{er} depends on the diameter of glass or aluminum particles (the density ρ_p here varies from 2500 to 2700 kg/m³) for the case of single particle impact over a range of particle impact speeds varying from 1000 to 5000 m/sec. The bulk of the points is for the impact onto glass Textolite; however, we show for comparison the results from [3] for experiments involving homogeneous glass targets and the results from [2] for aluminum targets. We see that for d_p in the range from 1 to 5 mm that H_{er} is practically independent of particle size, whereas, in going over to micron-sized particles (from 0.4 to 5 μm), the magnitude of the effective enthalpy turns out to be an order of magnitude higher.

It is of interest to compare the data of Fig. 4 with the value of the effective damage enthalpy I_{eff} in the case of thermochemical action of a gaseous flow [see Eq. (1)]. It is well known, for glassy materials of quartz glass type, that

$$I_{eff} = c\,(T_w - T_0) + \Gamma\,[\Delta Q_{vap} + \gamma\,(I_e - I_w)],$$

i.e., the effective enthalpy is made up of heat, which goes toward the heating and melting of the material, $(\Delta Q_h + \Delta Q_m) = c(T_w - T_0)$, as well as the vaporization ΔQ_{vap} and blowing in the boundary layer $\gamma(I_e - I_w)$ of the fraction (Γ) of the eroded mass. For single-particle impact the thermal effect of blowing is, of course,

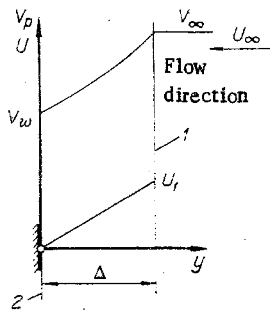

Fig. 6

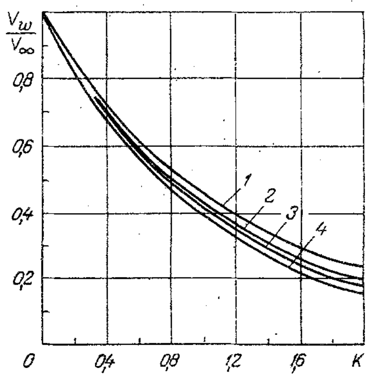

Fig. 7

Fig. 6. Schematic for the motion of a particle in the shock layer: 1) the shock wave; 2) surface of the target.

Fig. 7. Influence of the parameter $K = 3/4C(\rho/\rho_p)(\Delta/d_p)$ on the degree of slowdown of a particle in a compressed gas layer of thickness Δ and density ρ: 1) $U_1/V_\infty = 0.2$; 2) $U_1/V_\infty = 0.15$; 3) $U_1/V_\infty = 0.1$; 4) $U_1/V_\infty = 0.05$.

absent; however, for ultrafine particles the quantity H_{er} is found to be close to the maximum possible thermodynamic enthalpy of quartz glass

$$\Delta Q_h + \Delta Q_m + \Delta Q_{vap} \approx 14000 \text{ kJ/kg}.$$

The more coarse the particles in relation to the characteristic scale of the target material structure, the more likely there will be mechanical break-off of the material but no vaporization of individual grains during the impact process. By taking note of an approximate equation for the heat of fusion and the energy required to break all the mechanical bonds, we can, subject to crude estimates, adopt the following range for the variation of H_{er} for glass plastics:

$$\frac{\varphi_f n}{3}[\Delta Q_h + \Delta Q_m] \leqslant H_{er} \leqslant [\Delta Q_h + \Delta Q_m + \Delta Q_{vap}], \tag{6}$$

where the factor φ_f on the left-hand side of Eq. (6) represents the fraction of glass fibers in the target material and also the degree of material strength in the three principal directions ($n = 3$ for isotropic three-dimensional glass plastics and $n = 1$ for anisotropic unwoven Textolites).

Figure 4 also shows experimental data for the values of the effective erosional damage enthalpy during multiple particle impact. Two circumstances present themselves here: There is practically no dependence of H_{er} on the particle diameter, and the value of the effective enthalpy during multiple impact is substantially less than that for single impact [it is close to the minimum level indicated by inequality (6)].

Thus, indeed, we have essentially transformed, both quantitatively and also qualitatively, the dependence in the case of multiple impact of the critical speed V_{crit} for erosional damage on the particle size (Fig. 2). However, we need, first of all, to make more precise what is meant in this case by the critical speed. In the case of multiple impact, there is probably no explicit threshold for the onset of erosional damage since with an infinite increase in the particle flow or the time of the experiment, no significant increase in the mass carried away is observed even in the case of very small speeds V_p. Therefore, by analogy with thermochemical damage, we assume that there is a value of $G_{crit} = \omega$ corresponding to the onset of erosional damage, where ω is a specified small positive number (in our case $\omega = 0.005$). It is also necessary that the erosional damage process has a stationary character, i.e., the quantity $\bar{\bar{G}}$ should not depend on the time of the experiment.

We now formulate a third condition for a calculational model, one which establishes a correspondence between the erosional damage processes for single and for multiple impacts.

For the same particle sizes and densities the ratio of the critical speeds for single and for multiple impacts, viz., $V_{crit}(1)/V_{crit}(n)$, is proportional to the square root of the ratio of the corresponding effective erosional damage enthalpies:

$$V_{crit}(1)/V_{crit}(n) \backsim \sqrt{\overline{H_{er}(1)}/\overline{H_{er}(n)}}. \quad (7)$$

This relationship can be justified by the fact that the effective enthalpy $H_{er}(n)$, as a characteristic of the energy for breaking of the bonds in the target material, must reflect the change in its capacity to deform elastically, such deformations taking place during the multiple bombardment of the surface (in particular, the formation of microcracks, a decrease in values of the flow limit and of the maximum elongation).

We can arrive at an analogous conclusion also from empirical relationships between the number of cracks and the strength of glass [10].

According to the Eqs. (4) and (7), in the case of multiple interaction, a lowering of the critical speed V_{crit} is observed with an increase in the particle diameter d_p for $d_p < 100\ \mu m$, while the effective enthalpy $H_{er}(1)$ is weakly dependent on the diameter d_p. Then, for large values of d_p, there is an essential lowering (in agreement with the data of Fig. 4) of the value of the effective enthalpy $H_{er}(1)$ and, consequently, almost a stoppage in the lowering of the speed V_{crit} (Fig. 2).

There is at present too little experimental data to assert that this frequency is maintained even for $d_p > 1$ mm, and not only for glass Textolites but also for other elastic materials.

In Fig. 5 we present calculated curves showing how the damage intensity $\bar{\bar{G}}$ depends on the impact speed for various particle diameters; we have also plotted experimental points for a number of glassy materials described in [8, 9].

It is evident that the calculated curves satisfactorily describe the basic tendencies in the variation of the erosional damage intensity with the two-phase flow speed V_p and also with the diameter d_p of the solid particles.

In conclusion, we go into some more detail concerning the gasdynamics of two-phase flow. As the previous analysis shows, it is necessary to determine the impact speed V_p of the particles with the target surface fairly accurately.

High particle speeds are attained in the case of a supersonic flow past a target, resulting in the formation of a shock wave in front of the blunted part of the target; behind this shock wave the particles are slowed substantially in a layer of compressed gas. In the majority of the experimental studies the speed of the particles is either generally not recorded or else the measurements are made in the unperturbed flow far from the target surface. Therefore, we give a simple engineering method for estimating this effect for a neighborhood of the stagnation point, which allows for a more precise treatment and a comparison of the results of the experimental studies.

The motion of a particle in the shock layer has certain features. We note, first of all, that the gas flow behind the straight shock wave is slowed down abruptly, its speed becomes subsonic, and the velocity profile through the thickness of the shock layer decreases practically linearly. Therefore, the particles in the shock layer always have a sufficiently large speed in relation to the slowed-down gas. In experimental gasdynamics the greatest interest attaches to those cases in which the particles arrive at the target surface with significant speed. Moreover, by virtue of the large Reynolds number, we can take the drag coefficients of the particles to be constant, equal for spheres to $C_d = 0.44$ in the case of subsonic flow and to $C_d \sim 1.0$ in the case of supersonic flow. If the particle shapes are nonspherical, then, to determine C_d we can use a number of semi-empirical relations, e.g., those given in [7].

The motion of a particle along the axial streamline in the shock layer is described by the equation (see Fig. 6)

$$\frac{dV_p}{d\bar{y}} = -K\frac{(V_p - U)^2}{V_p}, \quad (8)$$

where $K = (C_d S\rho/2m_p)\Delta$ [$K = (3/4)C_d(\rho/\rho_p)(\Delta/d_p)$ for a sphere]; $U = U_1\bar{y}$, where $\bar{y} = y/\Delta$ is the coordinate in the shock layer of thickness Δ for a gas of density ρ; V_p, U, speed of the particle and also of the gas; m_p, ρ_p, and S, respectively, the mass, the density, and the midsection area of the particle.

For $U/V_p < 0.3$ this equation may be approximated with good accuracy by the linear equation

$$\frac{dV_p}{d\bar{y}} - KV_p = -1.75KU_1\bar{y}, \quad (9)$$

which has the simple solution

$$\frac{V_p}{V_\infty}=\frac{1.75U_1}{KV_\infty}\left[\left(\frac{KV_\infty}{1.75U_1}-K-1\right)\exp\left(K\left(\bar{y}-1\right)\right)+K\bar{y}+1\right]. \tag{10}$$

It follows from (10) that the particle speed at the surface is determined by putting y = 0:

$$\frac{V_w}{V_\infty}=\frac{1.75U_1}{KV_\infty}\left[\left(\frac{KV_\infty}{1.75U_1}-K-1\right)\exp\left(-K\right)+1\right]. \tag{11}$$

This equation is shown graphically in Fig. 7.

If in the incident flow the particles and the gas are in a state close to equilibrium, then the Mach number, starting with which the condition $U/V_p < 0.3$ is satisfied behind the shock wave, is determined from the relation

$$M=\sqrt{\frac{2.86}{1.86-\varkappa}},$$

where $\varkappa$ is the isentropic exponent.

By way of an example, we determine the speed of a spherical particle of diameter $d_p = 10^{-4}$ m and of density $\rho_p = 2500$ kg/m^3 close to the surface of a target after a flight with initial speed $V_\infty = 1500$ m/sec through a shock layer of thickness $\Delta = 2\cdot 10^{-2}$ m and density $\rho = 5$ kg/m^3; the speed of the gas behind the shock wave is $U_1 = 300$ m/sec. For this data we easily calculate that $K = 0.3$ and that $U_1/V_\infty = 0.2$. Using Fig. 7, we find that $V_w/V_\infty = 0.78$ and that $V_w = 1170$ m/sec. Obviously, it is necessary to take such a change in particle speed into account when treating experimental results.

If in the motion of a spherical particle through the shock layer two consecutive flow regimes are realized, viz., a supersonic flow and then a subsonic flow with different C_d values, then the determination of the particle speed at the surface must be made in two steps. First, we need to find the coordinate $\bar{y}$ at which the particle is slowed to the speed of sound. For this we use equation (10), written in the form

$$\Phi=\Phi(0)\exp(K\bar{y})+K\bar{y}, \tag{12}$$

where

$$\Phi=\frac{KV_p}{1.75U_1}-1,\quad \Phi(0)=\frac{KV_w}{1.75U_1}-1.$$

With an accuracy sufficient for practical purposes, the solution of this equation is given by the relation

$$\bar{y}=\frac{1}{K}\ln\frac{\Phi-\ln\dfrac{\Phi}{\Phi(0)}}{\Phi(0)}. \tag{13}$$

Then, knowing the coordinate $\bar{y}$, we determine the speed to which the particle is slowed on the remaining portion of its trajectory as would be done for a new shock layer.

NOTATION

U and V	are the velocities of gas and particle, respectively;
G	is the specific mass flow;
$\bar{G}$	is the dimensionless thermochemical damage rate;
$\bar{\bar{G}}$	is the relative damage intensity;
H_{er}	is the effective enthalpy of eroded mass;
H_{B_0}	is the Brinell hardness;
I_{eff}	is the effective damage enthalpy;
I_e, I_w	are the enthalpy at incident flow and surface temperatures;
$(\alpha/c_p)_0$	is the heat-transfer coefficient;
ε	is the emissivity;
σ	is the Stefan–Boltzmann constant;
T	is the temperature;
ρ	is the density;

σ_T	is the yield limit;
d	is the diameter;
c	is the heat capacity;
Γ	is the fraction of vaporized material;
γ	is the blowing coefficient;
ΔQ_m, ΔQ_{vap}	are the specific heats of fusion and vaporization;
φ_f	is the glass fiber fraction in target material;
ω	is the specified small positive number;
Re	is the Reynolds number;
C_d	is the drag coefficient;
m	is the mass;
S	is the midsection area;
Δ	is the shock layer thickness;
$\bar{y}$	is the shock layer coordinate;
M	is the Mach number;
$\varkappa$	is the isentropic exponent;
K, Φ	are the quantities defined following Eqs. (8) and (12), respectively;

Subscripts

∞, 1, and w	relate to the ambient flow, the flow behind the shock wave, and the flow at the target surface, respectively;
subscripts p and 0	relate to the particle and the target wall, respectively;
subscripts er and k	are for erosion and thermochemical damage, respectively;
subscript crit	refers to the critical velocity.

LITERATURE CITED

1. R. J. Eichelberger and J. H. Kineke, Jr., "Hypervelocity impact," in: Short-Time Physics, Springer-Verlag, Vienna (1967), pp. 659-692.
2. L. V. Leont'ev, "On the shape of craters formed during high velocity impact," Kosm. Issled., 14, No. 2 (1976).
3. J. F. Vedder and J.-C. Mandeville, "Microcraters formed in glass by projectiles of various densities," J. Geophys. Res., 79, 3247-3256 (1974).
4. Yu. V. Polezhaev and F. B. Yurevich, Heat Shield [in Russian], Énergiya, Moscow (1976).
5. W. Goldsmith, "Impact: the collision of solids," Appl. Mech. Rev., 16, 855-866 (1963).
6. A. T. Bazilevskii and B. A. Ivanov, "A survey of progress in the mechanics of crater formation," in: Mechanics. New Developments in Foreign Science [in Russian], Vol. 12, A. Yu. Ishlinskii and G. G. Chernyi (editors), Mir, Moscow (1977).
7. I. P. Vereshchagin, V. I. Levitov, G. Z. Mirzabekyan, and M. M. Pashin, Fundamentals of Electrogasdynamic Disperse Systems [in Russian], Énergiya, Moscow (1974).
8. G. P. Tilly, Wear, 14, No. 1, 63-79 (1969).
9. G. P. Tilly and W. Sage, Wear, 16, No. 6, 447 (1970).
10. S. S. Solntsev and E. M. Morozov, Fracture of Glass [in Russian], Mashinostroenie, Moscow (1978).